CDF/ANAL/EXOTIC/PUBLIC/9302
Version 3.0

Search for Technicolor Particles Produced in Association with $W^{\pm}$ Boson with 1.9 fb^{-1} at CDF

The CDF Collaboration
http://www-cdf.fnal.gov
(Dated: April 27, 2008)

We present a search for technicolor particles decaying into $b\bar{b}$, $b\bar{c}$ or $b\bar{u}$ and produced in association with W bosons in $p\bar{p}$ collisions at $\sqrt{s} = 1.96\,\text{TeV}$. The search uses approximately $1.9\,\text{fb}^{-1}$ of the dataset accumulated in the CDF detector at the Fermilab Tevatron. We select events matching the W + 2-jets signature and require at least one jets to be identified as b-quark jets. In the case of exactly one vertex b-tagged events, we apply a neural network flavor separator to reject contamination from charm and light quark jets. The number of tagged events and the invariant mass distributions of $W + 2$ jets and dijets are consistent with the Standard Model expectations. We set a 95% confidence level excluded region on the production cross section times branching ratio as a function of the technicolor particle masses.

Preliminary results for Winter 2008 conferences

I. INTRODUCTION

The mechanism of electroweak symmetry breaking in the standard model is still unknown. Two of the most popular mechanisms to induce spontaneous symmetry breaking of the gauge theory, resulting in massive gauge bosons and fermions, are the Higgs mechanism and the dynamics of a new interaction such as technicolor [1, 2]. Both mechanisms predict the existence of new particles which could be produced at the Tevatron in association with a W boson.

Here we present a search for technirho production in $p\bar{p}$ collisions at $\sqrt{s} = 1.96\,\text{TeV}$ with subsequent decay to technipions (Fig 1). The signatures we focus on are $p\bar{p} \to \rho_T^{\pm} \to W^{\pm}\pi_T^0 \to \ell\nu b\bar{b}$ and $p\bar{p} \to \rho_T^0 \to W^{\pm}\pi_T^{\mp} \to \ell\nu b\bar{c}, \ell\nu b\bar{u}$. The production cross secion of these processes is the order picobarns (Fig. 2) [3].

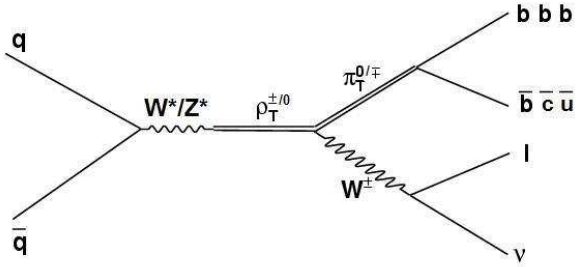

FIG. 1: Feynman diagram for $p\bar{p} \to \rho_T^{\pm/0} \to W^{\pm}\pi_T^{0/\mp} \to \ell\nu b\bar{b}$, $\ell\nu b\bar{c}$ or $\ell\nu b\bar{c}$ production.

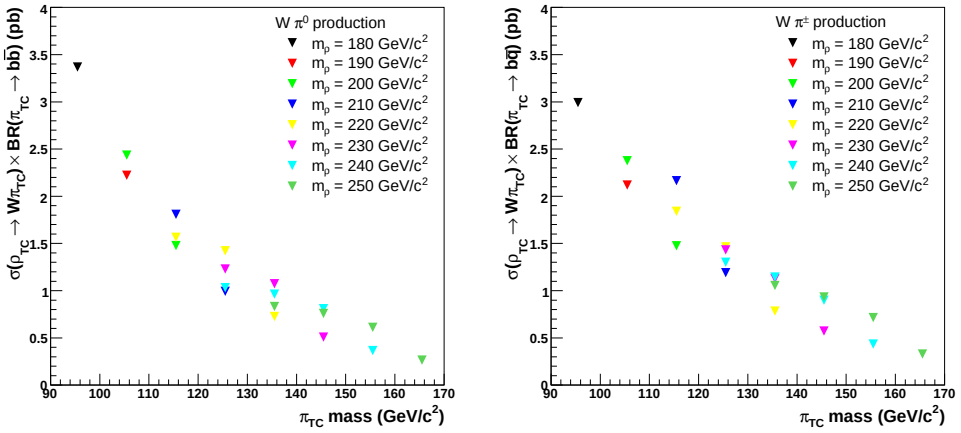

FIG. 2: Production cross section calculated in PYTHIA 6.216 with the Technicolor Straw Model (TCSM). (Left) $p\bar{p} \to \rho_T^{\pm} \to W^{\pm}\pi_T^0 \to \ell\nu b\bar{b}$ production cross section as a function of the technipion mass for various technirho masses. (Right) $p\bar{p} \to \rho_T^0 \to W^{\pm}\pi_T^{\mp} \to \ell\nu b\bar{c}$, $\ell\nu b\bar{u}$ production cross section as a function of the technipion mass for various technirho masses.

The final state from $W\pi_T$ production is high-p_T lepton, large missing transverse energy ($\not\!\!E_T$) and one or two b-jets.

The previous search at CDF [4] was performed in a dataset with integrated luminosity equivalent to $955\,\text{pb}^{-1}$. Other searches at Tevatron have been published using data collected at the DØ detector [5]. The search for technicolor particle were also performed at LEP [6]. They only excluded technirho mass less than 206.7GeV due to the LEP beam energy restriction.

II. DATA SAMPLE & EVENT SELECTION

We use the data collected through May 2007, corresponding to an integrated luminosity $1.9\,\mathrm{fb}^{-1}$. The events are collected by the CDF II detector with high-p_T electron or muon triggers [7] ,which can detect electrons or muons with E_T or $p_T > 18$GeV. We further require the electron or muon that is isolated with E_T or $p_T > 20$GeV at offline level.

To select the W + 2jet final state, we require that events have the large missing transverse energy and one or two b-jets. Therefore, we require that events have $\not\!\!E_T > 20$GeV and exactly two jets ,where jets are defined using a cone algorithm with radius 0.4. We count jets which have $E_T > 20$GeV and $|\eta| < 2.0$.

To reduce the background, we require that at least one jet in the event are identified as b-jet by the Secondary Vertex Tagging Algorithm. The secondary vertex tagging algorithm identifies b-jets by fitting tracks displaced from the primary vertex. This method has been used by other Higgs searches and top analyses at CDF [8, 9]. In Addition, we add the Jet Probability Tagging Algorithm that identifies b-jets by requireing a low probability that all tracks contained in a jet originated from the primary vertex, based on the track impact parameters [10]. To be considered for double tag category, we require that events have two secondary vertex tags or one secondary vertex tag and one jet probability tag.

To increase the signal acceptance, we also make use of the exactly one b-tagged events with secondary vertex tagging algorithm. For the exactly one b-tagged events, we apply the neural network b-tagging algorithm to improve signal-to-background ratio. This neural network b-tagging algorithm is used in previous analysis [4, 9]. With using this algorithm, we can improve the purity of b-jets while keeping about 90% signal.

The dijet mass is reconstructed from the 2 jets in selected events. To reconstruct the W + 2jets invariant mass, we need to determine the p_z of the neutrino from the W boson. After using the W mass constraint to solve for the kinematics of the $\ell\nu$ system, we take a smaller value of the two p_z solutions. (If there is no real solution for p_z, we take the real part of the complex solution.)

III. SIGNAL ACCEPTANCE

The signal acceptance is calculated using technicolor events generated with the PYTHIA program [11]. PYTHIA version 6.216 implements the Technicolor Straw Man Model [3] in leading-order calculations. We set the mass parameters as $M_V = M_A = 200\,\mathrm{GeV}/c^2$, the charge of up-type technifermion as $Q_U = 1$ and the mixing angle between isotriplet technipion interaction and mass eigenstates as $sin\chi = 1/3$ in this model. For this study, we focus on the mass region as:

$$m(W) + m(\pi_T) < m(\rho_T) < 2 \times m(\pi_T) \tag{1}$$

$$180\mathrm{GeV}/c^2 < m(\rho_T) < 250\mathrm{GeV}/c^2$$

$$95\mathrm{GeV}/c^2 < m(\pi_T) < 165\mathrm{GeV}/c^2$$

because of the kinematical threshold of $W\pi_T$ production and pair π_T production.

Figure 3-4 show the acceptance as a function of $m(\pi_T)$ for each $m(\rho_T)$ for neutral and charged technipi channel. The acceptance includes various calibration scale factors quantifying the difference between simulation and data, and it includes the efficiency of the high p_T-lepton triggers. No K-factor is applied to the leading-order calculation of the acceptance and cross section.

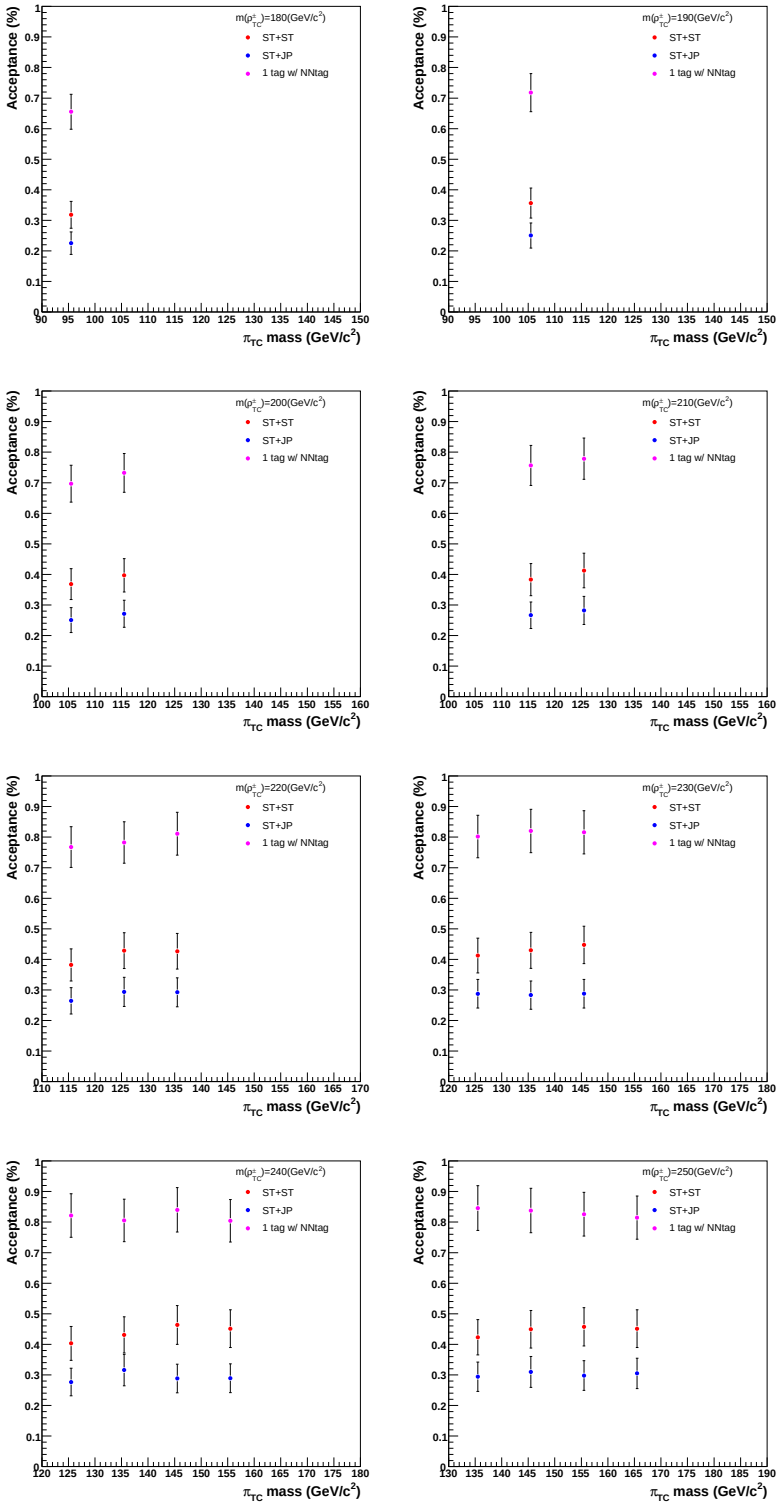

FIG. 3: Technicolor signal acceptance for neutral technipi channel as a function of technipion mass $m(\pi_T)$ for each technirho mass $m(\rho_T)$. The three different selections – exactly one secondary vertex tag with NN b-tag, double secondary vertex tag or one secondary vertex tag plus one jet probability tag – are shown in magenta, red and blue, respectively.

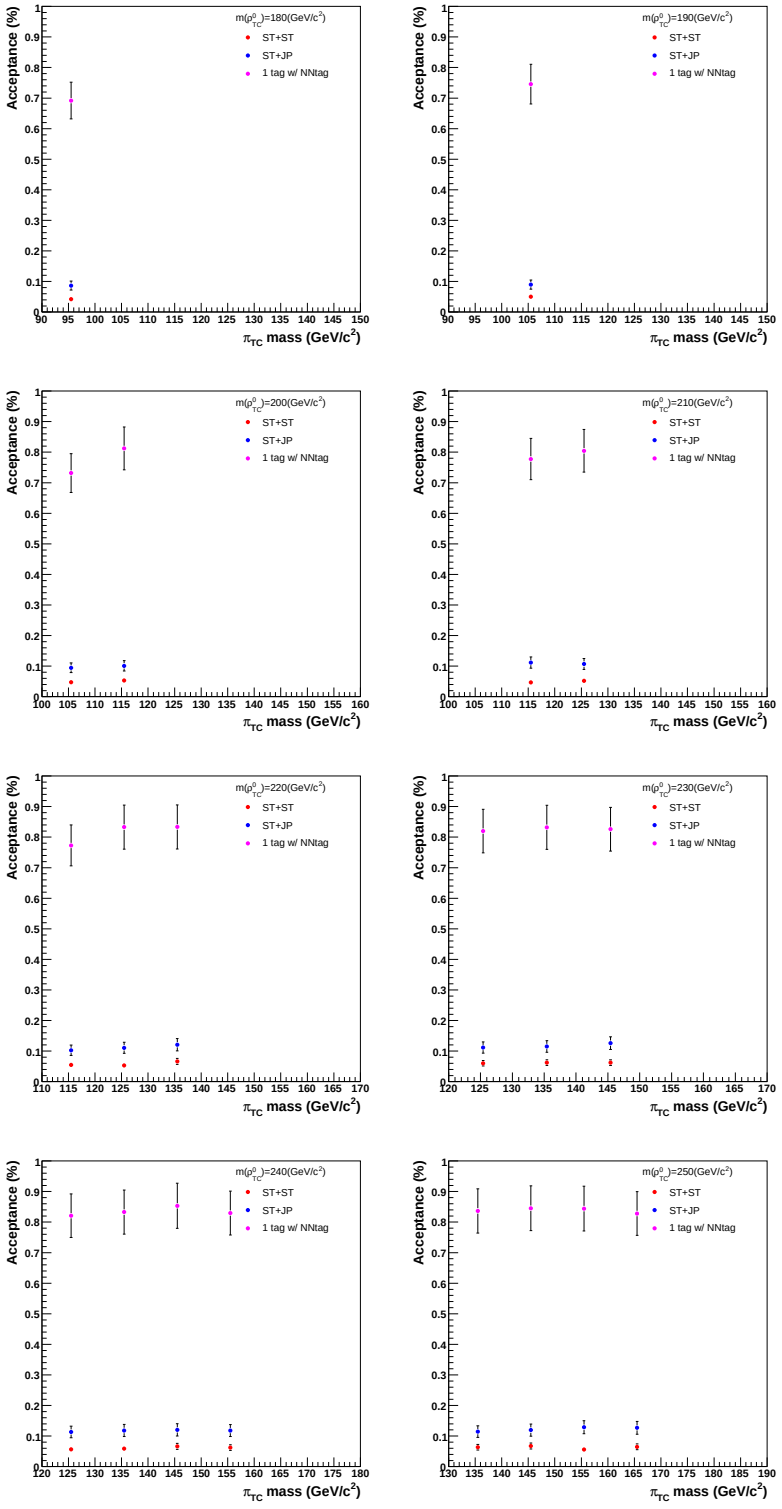

FIG. 4: Technicolor signal acceptance for charged technipi channel as a function of technipion mass $m(\pi_T)$ for each technirho mass $m(\rho_T)$. The three different selections – exactly 1 one secondary vertex tag with NN b-tag, double secondary vertex tag or one secondary vertex tag plus one jet probability tag – are shown in magenta, red and blue, respectively.

b-tagging category	LeptonID	Trigger	ISR/FSR	JES	PDF	b-tagging	Total
One tag w/ NN tag	$\sim 2\%$	$< 1\%$	2.4/1.8%	2.7%	2.3%	4.3%	6.7%
ST + ST	$\sim 2\%$	$< 1\%$	5.5/3.0%	3.8%	3.4%	8.4%	11.9%
ST + JP	$\sim 2\%$	$< 1\%$	4.6/3.3%	4.0%	3.6%	9.2%	12.2%

TABLE I: Summary of systematic uncertainties in the technicolor signal acceptance for the neutral technipi channel.

b-tagging category	LeptonID	Trigger	ISR/FSR	JES	PDF	b-tagging	Total
One tag w/ NN tag	$\sim 2\%$	$< 1\%$	3.2/2.3%	3.4%	3.0%	4.3%	7.7%
ST + ST	$\sim 2\%$	$< 1\%$	11.6/8.3%	11.3%	3.8%	9.4%	21.0%
ST + JP	$\sim 2\%$	$< 1\%$	8.0/5.1%	5.9%	3.8%	17.0%	20.8%

TABLE II: Summary of systematic uncertainties in the technicolor signal acceptance for the charged technipi channel.

Systematic uncertainties from the b-tagging efficiency, initial and final state radiation effects (ISR/FSR), parton distribution function (PDF) and the jet energy scale (JES) are also considered. The summarized systematic uncertainties are shown in Table I-II.

IV. BACKGROUND ESTIMATES

This analysis builds on the method of background estimation detailed in Ref. [8]. In particular, the contributions from the following individual backgrounds are calculated: falsely b-tagged events (mistag), W production with heavy flavor quarks ($W + b\bar{b}$, $W + c\bar{c}$, $W + c$), QCD events with false W signatures, top quark pair or single production and diboson production (WW, WZ, ZZ).

We estimate the mistag events by using the mistag probability that measured from the inclusive jets sample. Such mistag rate are obtained using negative tags, which are the tags that appear to travel back toward the primary vertex. The mistag rate derived from negative tags is due to tracking resolution limitations, but they provide a reasonable estimate of the number of false positive tags after a correction for material interactions and long-lived light flavor particles.

The number of events from W + heavy flavor is calculated using information from both data and Monte Carlo samples. We calculate the fraction of W events with associated heavy flavor production in the ALPGEN Monte Carlo program interfaced with the PYTHIA parton shower code [11, 12]. This fraction and the tagging efficiency for such events are applied to the number of events in the original W+jets sample after correcting for the $t\bar{t}$ and electroweak contributions.

We constrain the number of QCD events with false W signatures by assuming the lepton isolation is independent of $\not\!\!E_T$ and measuring the ratio of isolated to non-isolated leptons in a $\not\!\!E_T$ sideband region. The result in the tagged sample can be calculated in two ways: by applying the method directly to the tagged sample, or by estimating the number of non-W QCD events in the pretag sample and applying an average b-tagging rate.

The summary of the background contributions to the double secondary vertex tagged events, the one secondary vertex plus one jet probability tagged events and the one secondary vertex tagged with neural network b-tag events are shown in Table III-V. Because the expected number of technicolor signal events is small in the 1-,3- and 4-jet bins, the reasonable agreement between predicted backgrounds and observed data gives us confidence in our overall background estimate.

Njet	2jet	3jet	>=4jet
Pretag Events	32242	5496	1494
Mistag	3.88±0.35	2.41±0.24	1.62± 0.14
$Wb\bar{b}$	37.93±16.92	14.05±5.49	7.39± 2.93
$Wc\bar{c}$	2.88±1.25	1.52±0.61	1.15± 0.47
$t\bar{t}$(6.7pb)	19.05±2.92	54.67±8.38	94.93± 14.56
Single top(s-ch)	6.90±1.00	2.28±0.33	0.61± 0.088
Single top(t-ch)	1.60±0.23	1.43±0.21	0.50± 0.07
WW	0.17±0.02	0.15±0.02	0.16± 0.02
WZ	2.41±0.26	0.68±0.07	0.16± 0.02
ZZ	0.06±0.01	0.06±0.01	0.02±0.001
$Z->\tau\tau$	0.25±0.04	0.19±0.03	0.06±0.01
nonW QCD	5.50±1.00	2.56±0.48	1.02± 0.22
Total Bkg	80.62±18.75	79.99±10.92	107.63± 15.15
m($\rho^{\pm}$,π^0)=(200,115) GeV	11.24±0.98	Control region	Control region
m(ρ^0,$\pi^{\mp}$)=(200,115) GeV	1.50±0.16	Control region	Control region
Observed Events	83	88	118

TABLE III: Background summary table for double secondary vertex tag category.

Njet	2jet	3jet	>=4jet
Pretag Events	32242	5496	1494
Mistag	11.73±0.92	8.11±0.64	8.39±0.58
$Wb\bar{b}$	31.15±14.03	11.47±4.55	6.55±2.63
$Wc\bar{c}$	7.87±3.43	4.38±1.76	3.09±1.27
$t\bar{t}$(6.7pb)	15.56±2.39	47.48±7.28	79.81±12.24
Single top(s-ch)	5.14±0.75	1.90±0.27	0.53±0.07
Single top(t-ch)	1.87±0.27	1.49±0.22	0.44±0.06
WW	0.93±0.11	0.63±0.08	0.47±0.06
WZ	1.84±0.20	0.59±0.06	0.19±0.02
ZZ	0.08±0.01	0.04±0.003	0.02±0.002
$Z->\tau\tau$	1.29±0.20	0.53±0.08	0.20±0.03
nonW QCD	9.55±1.73	4.87±0.93	1.80±0.40
Total Bkg	86.99±17.99	81.46±10.22	101.49±13.08
m($\rho^{\pm}$,π^0)=(200,115) GeV	7.69±0.87	Control region	Control region
m(ρ^0,$\pi^{\mp}$)=(200,115) GeV	2.85±0.34	Control region	Control region
Observed Events	90	80	106

TABLE IV: Background summary table for one secondary vertex tag + one jet probability tag category.

Njet	1jet	2jet	3jet	>=4jet
Pretag Events	196160	32242	5496	1494
Mistag	236.7±19.36	107.1±9.38	41.84±3.839	20.97±1.91
$Wb\bar{b}$	431.7±182.4	215.6±92.34	61.78±24.68	26.14±10.43
$Wc\bar{c}$	514.4±154.7	167±62.14	45.4±15.31	17.71±6.86
$t\bar{t}$(6.7pb)	11.85±1.82	60.68±9.30	111±17.03	122.4±18.76
Single top(s-ch)	7.09±1.03	14.38±2.09	3.91±0.57	0.97±0.14
Single top(t-ch)	23.31±3.41	29.57±4.33	6.24±0.91	1.11±0.16
WW	7.21±0.89	15.45±1.91	4.61±0.57	1.03±0.13
WZ	5.52±0.59	7.59±0.81	1.76±0.19	0.48±0.05
ZZ	0.17±0.02	0.31±0.03	0.14±0.01	0.07±0.01
$Z->\tau\tau$	14.58±2.25	7.27±1.12	2.39±0.37	0.71±0.11
nonW QCD	465±83.21	184.7±33.04	44.83±8.57	17.03±3.67
Total Bkg	1717.6±347.89	809.61±159.38	323.92±45.45	208.57±26.24
m($\rho^{\pm}$,π^{0})=(200,115) GeV	Control region	20.74 ± 1.61	Control region	Control region
m(ρ^{0},$\pi^{\mp}$)=(200,115) GeV	Control region	22.96±1.78	Control region	Control region
Observed Events	1812	805	306	215

TABLE V: Background summary table for one secondary vertex tag with NN tag category.

V. RESULTS

We perform a direct search for a resonant mass peak in the reconstructed W + 2-jet and dijet invariant mass distributions from the single-tagged and double-tagged events. In fact, we consider the dijet mass distribution and the Q-value defined as $Q = m(\rho_T) - m(\pi_T) - m(W)$. The observed data spectra for these variables are consistent with the background estimate, as shown in Figs. 5-7.

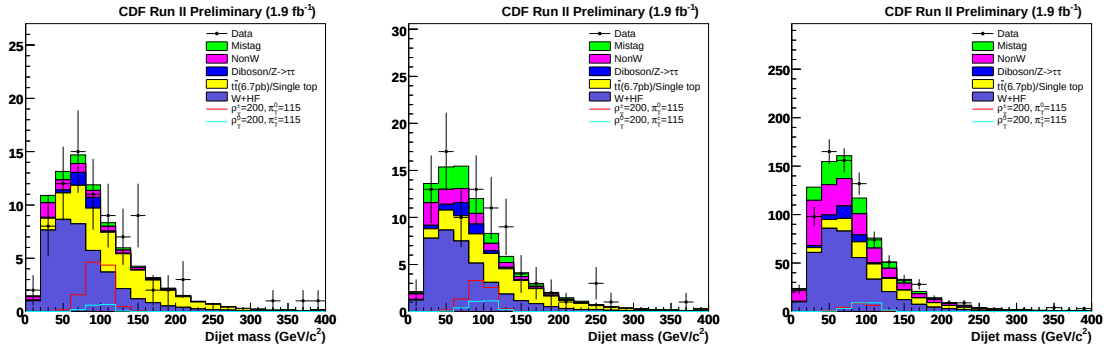

FIG. 5: Distributions of the dijet invariant masses for the predicted and observed data. Results are shown for the double secondary vertex tag (left), the one secondary vertex tag + one jet probability tag (middle) and the one secondary vertex tag with NN tag (right).

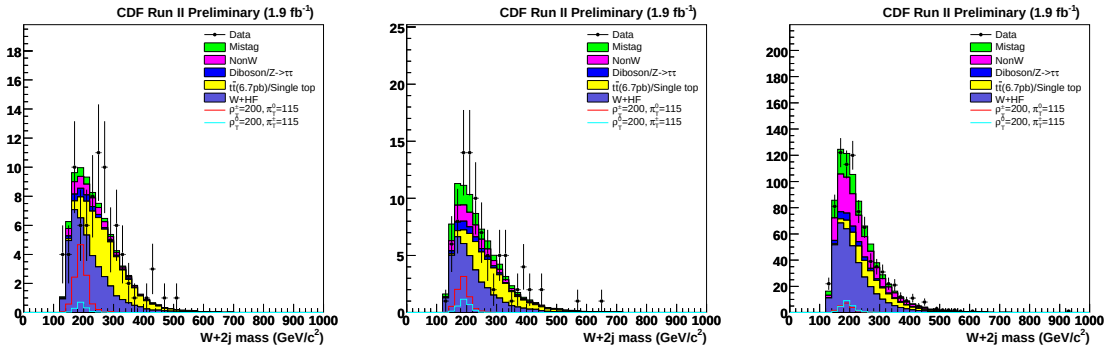

FIG. 6: Distributions of the W + 2-jets invariant masses for the predicted and observed data. Results are shown for the double secondary vertex tag (left), the one secondary vertex tag + one jet probability tag (middle) and the one secondary vertex tag with NN tag (right).

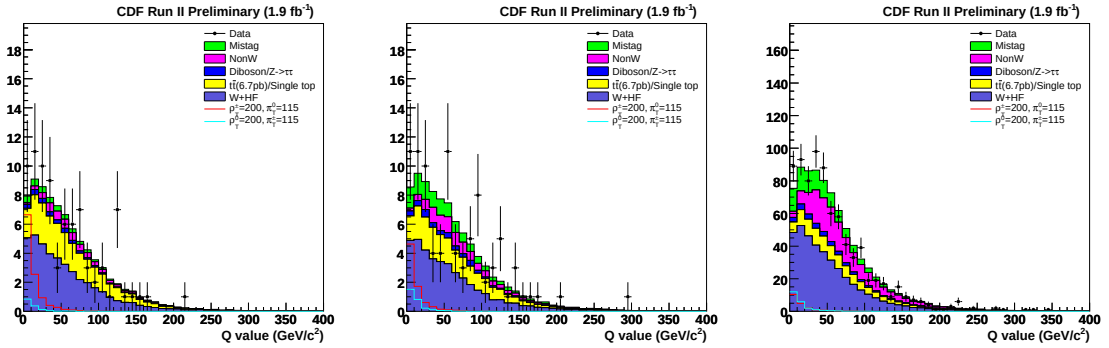

FIG. 7: Distributions of the final Q-value for the predicted and observed data. Results are shown for the double secondary vertex tag (left), the one secondary vertex tag + one jet probability tag (middle) and the one secondary vertex tag with NN tag (right).

Since there is no significant excess of events in the data compared to the predicted background, we set the 95% C.L. excluded region on technicolor production as a function of the technicolor particles mass. A 2-dimensional binned maximum likelihood technique is used on the 2-dimensional distribution of dijet invariant mass vs Q-value by constraining the number of background events within the uncertainties. Figs. 8-10 show the 2-dimensional distribution of data, backgrounds and signal for each tag category.

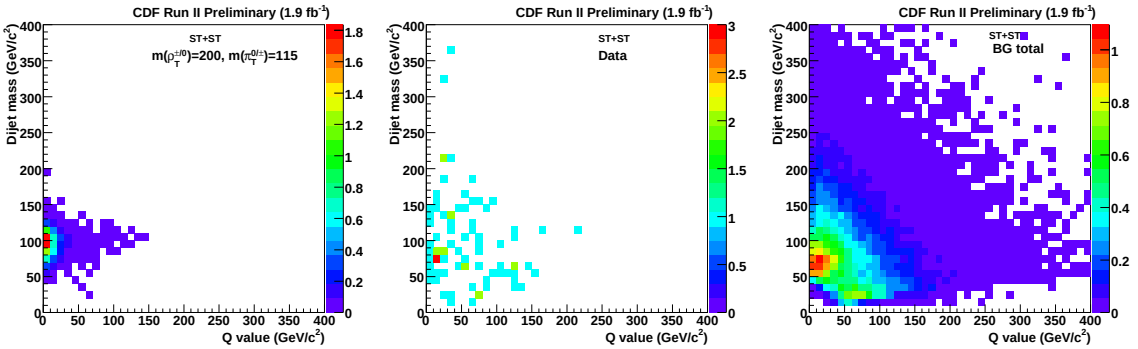

FIG. 8: Dijet mass vs Q value 2-dimensional distribution of signal MC (left, $m(\rho_T) = 200\text{GeV/c}^2$, $m(\pi_T) = 115\text{GeV/c}^2$), data (middle) and backgrounds (right) for the double secondary vertex tag category.

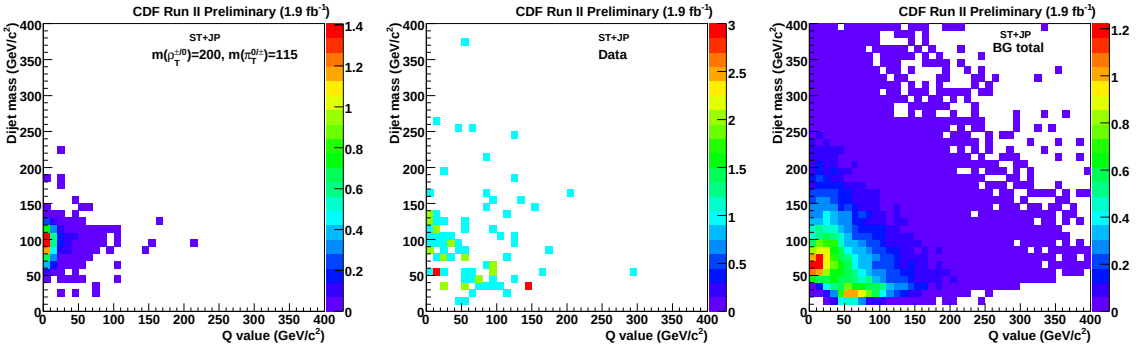

FIG. 9: Dijet mass vs Q value 2-dimensional distribution of signal MC (left, $m(\rho_T) = 200\text{GeV/c}^2$, $m(\pi_T) = 115\text{GeV/c}^2$), data (middle) and backgrounds (right) for the one secondary vertex tag + one jet probability tag category.

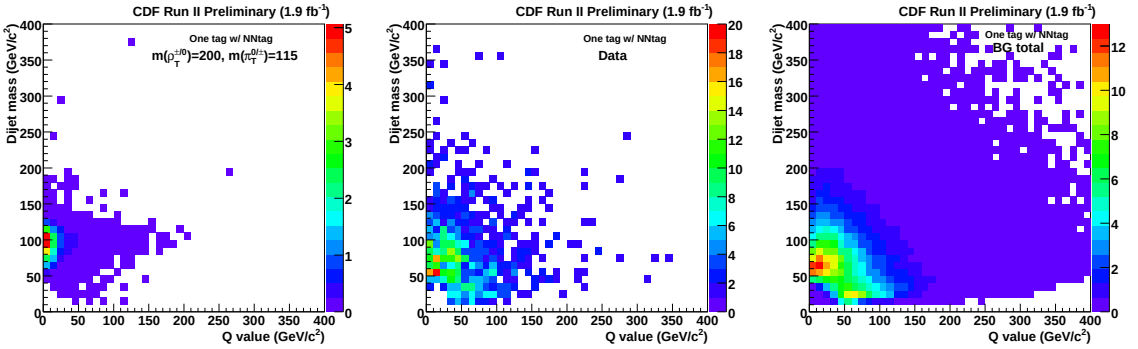

FIG. 10: Dijet mass vs Q value 2-dimensional distribution of signal MC (left, $m(\rho_T) = 200\text{GeV/c}^2$, $m(\pi_T) = 115\text{GeV/c}^2$), data (middle) and backgrounds (right) for the one secondary vertex tag with NN tag category.

The final expected and observed excluded region at 95% C.L. are shown in Fig. 11. A region of $m(\rho_T)$ = 180 - 250GeV are excluded at 95% C.L. based on the Technicolor Straw Man Model, except the region which are near the $W\pi_T$ production threshold with $m(\rho_T) \geq 220$GeV and $m(\pi_T) \geq 125$GeV.

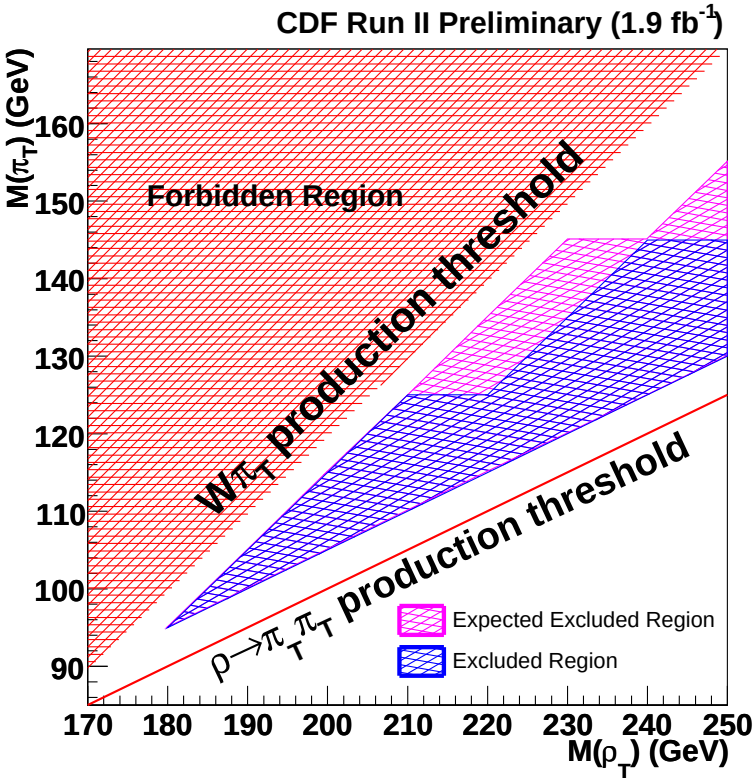

FIG. 11: The expected and observed excluded region at 95% C.L. as a function of technirho mass and technipi mass. Kinematical threshold of $W\pi_T$ and $\rho_T \to \pi_T\pi_T$ are shown in the figure.

$m(\rho_T)$	$m(\pi_T)$ exclude region at 95% C.L.
180 GeV	$m(\pi_T) = 95$ GeV
190 GeV	$m(\pi_T) = 105$ GeV
200 GeV	$105 < m(\pi_T) < 115$ GeV
210 GeV	$115 < m(\pi_T) < 125$ GeV
220 GeV	$115 < m(\pi_T) < 125$ GeV
230 GeV	$125 < m(\pi_T) < 135$ GeV
240 GeV	$125 < m(\pi_T) < 145$ GeV
250 GeV	$135 < m(\pi_T) < 145$ GeV

TABLE VI: The excluded region at 95% C.L in the ($m(\rho_T)$-$m(\pi_T)$) plane for $\rho_T \to W\pi_T \to l\nu b\bar{q}$ production

VI. CONCLUSIONS

We have performed a search for technicolor production $p\bar{p} \to \rho_T^{\pm/0} \to W^{\pm}\pi_T^{0/\mp} \to \ell\nu b\bar{b}$, $\ell\nu b\bar{c}$ or $\ell\nu b\bar{u}$ with the CDF II detector. We find that the dataset corresponding to $1.9\,\mathrm{fb}^{-1}$ agrees with the background predictions within uncertainties. A large region of $m(\rho_T) = 180$ - 250GeV and $m(\pi_T) = 95$ - 145GeV are excluded at 95% CL, based on the Technicolor Straw Man model (Table VI).

VII. ACKNOWLEDGEMENTS

We thank Ken Lane for helpful discussions, the Fermilab staff and the technical staffs of the participating institutions for their vital contributions. This work was supported by the U.S. Department of Energy and National Science Foundation; the Italian Istituto Nazionale di Fisica Nucleare; the Ministry of Education, Culture, Sports, Science and Technology of Japan; the Natural Sciences and Engineering Research Council of Canada; the National Science Council of the Republic of China; the Swiss National Science Foundation; the A.P. Sloan Foundation; the Bundesministerium für Bildung und Forschung, Germany; the Korean Science and Engineering Foundation and the Korean Research Foundation; the Particle Physics and Astronomy Research Council and the Royal Society, UK; the Russian Foundation for Basic Research; the Comision Interministerial de Ciencia y Tecnologia, Spain; and in part by the European Community's Human Potential Programme under contract HPRN-CT-20002, Probe for New Physics.

[1] S. Weinberg, "Implications of Dynamical Symmetry Breaking: An Addendum" Phys. Rev. **D19** (1979) 1277-1280.
L. Susskind, "Dynamics of Spontaneous Symmetry Breaking in the Weinberg-Salam Theory," Phys. Rev. **D20** strand, P. Ed n, C. Friberg, L. L (1979) 2619-2625.

[2] K. D. Lane, "Technihadron production and decay in low-scale technicolor" Phys. Rev. **D60** (1999) 075007, arXiv:hep-ph/9903369.

[3] K. Lane and S. Mrenna, "The collider phenomenology of technihadrons in the technicolor Straw Man Model" Phys. Rev. **D67** (2003) 115011, arXiv:hep-ph/0210299.

[4] CDF Collaboration, "Search for Technicolor Particles Produced in Association with W Bosons at CDF " CDF/ANAL/EXOTIC/PUBLIC/8566.

[5] DØ Collaboration, "Search for Techniparticles in e+jets events at D0" Phys. Rev. Lett. **98** 221801 (2007), arXiv:hep-ex/0612013.

[6] DELPHI Collaboration, "Search for Technicolor with DELPHI" Eur. Phys. J. **C22** 17 (2001), arXiv:hep-ex/0110056.

[7] F. Abe, *et al.*, Nucl. Instrum. Methods Phys. Res. A **271**, 387 (1988);
D. Amidei, *et al.*, Nucl. Instum. Methods Phys. Res. A **350**, 73 (1994);
F. Abe, *et al.*, Phys. Rev. D **52**, 4784 (1995);
P. Azzi, *et al.*, Nucl. Instrum. Methods Phys. Res. A **360**, 137 (1995);
The CDF II Detector Technical Design Report, Fermilab-Pub-96/390-E.
[8] A. Abulencia *et al.*, Phys. Rev. **D71**, 072005 (2005).
[9] T. Aaltonen *et al.*, Phys. Rev. Lett. **100** 041801 (2008).
[10] D. Buskulic, *et al.* (ALEPH Collaboration), Phys. Lett. B **313**, 535 (1993);
F. Abe *et al.* (CDF Collaboration), Phys. Rev. D **53**, 1051 (1996);
A. Affolder *et al.* (CDF Collaboration), Phys. Rev. D **64**, 032002 (2001);
Erratum-ibid: Phys. Rev. D **67**, 119901 (2003).
[11] T. Sjöstrand *et al.*, "High-Energy-Physics Event Generation with PYTHIA 6.1," Computer Physics Commun. **135** (2001) 238, arXiv:hep-ph/0010017
[12] M.L. Mangano *et al.*, "ALPGEN, a generator for hard multiparton processes in hadronic collisions," JHEP **0307**:001,2003, arXiv:hep-ph/0206293.
[13] G. Corcella *et al.*, "HERWIG 6.5: an event generator for Hadron Emission Reactions With Interfering Gluons," JHEP **0101** (2001) 010, arXiv:hep-ph/0011363